J|A|C|S
COMMUNICATIONS

Published on Web 01/27/2007

Highly Luminescent Quantum-Dot Monoliths

Indika U. Arachchige and Stephanie L. Brock*

Department of Chemistry, Wayne State University, Detroit, Michigan 48202

Received September 19, 2006; E-mail: sbrock@chem.wayne.edu

Through the exploitation of their unique and size dependent optical and electronic properties, quantum dots (QDs) promise to contribute to the advancement of a wide range of technologies ranging from LEDs and optical gain applications,[1] to biological labels, photovoltaic devices, and sensors.[2] Much effort has focused on developing syntheses that result in highly luminescent discrete semiconducting nanoparticles with excellent control of size, shape, and polydispersity.[3] However, with the exception of biological applications (sensing, imaging) most of the technologies envisioned are not single-particle based and will not operate in solution. Hence, developing methods for the assembly of QDs into solid-state architectures and understanding how the behavior of the individual dots is altered by the characteristics of the assembly are important challenges.

The majority of strategies employed for nanoparticle assembly involve either self-assembly to form superlattices (exploiting Van der Waals or electrostatic forces)[4] or the use of bifunctional ligands (covalent bonding).[5] In each of these cases, organic groups act as spacers between the particles, moderating their interactions, and the scale of the interconnected assembly is typically limited to micrometers. The ability to prepare large (mm−cm) assemblies of interconnected metal chalcogenide particles without the presence of intervening ligands has recently been realized by a sol−gel methodology.[6] QD networks of PbS, CdSe, CdS, and ZnS were prepared by oxidative removal of thiolate capping groups on the particle surface. The resultant gels were dried supercritically to prepare highly porous aerogels or on the benchtop to form more dense xerogels. Importantly, the extent of particle interaction in the network (the extent of quantum confinement) is a direct function of the dimensionality of the network, itself controlled by the density.[6] Aerogels (low density/dimensionality) are spectrally very similar to the precursor nanoparticles (highly confined), whereas xerogels show hardly any quantum confinement at all. Unfortunately, the photoluminescence properties of the resultant monoliths were weak (not detectible by eye), which was attributed to the presence of a large number of trap states at the network surface.[6] Highly luminescent monoliths have been formed by embedding quantum dots in a silica matrix using an organic hybrid sol−gel method, but the concentration of QDs that can be incorporated is limited.[7] In the present work, we show that highly luminescent QD monolith assemblies with varying porosity can be prepared by employing CdSe/ZnS core/shell nanoparticles as primary building blocks in sol−gel reactions. Furthermore, unlike the "naked" nanoparticle networks prepared earlier, the new composite structures are highly quantum confined, regardless of the density.

CdSe core nanoparticles with varying sizes were synthesized using arrested precipitation strategies and capped with ZnS using a modified literature preparation (Supporting Information).[8] These nanocrystals were surface exchanged with 11-mercaptoundecanoic acid (MUA) and dissolved in methanol to make highly luminescent CdSe/ZnS sols. Three different sizes of nanoparticles were prepared: orange particles with a yellow-green emission at 549 nm (∼4.4 nm CdSe core); red particles with an orange emission at 574 nm (∼5.1 nm CdSe core); and brown particles with a red emission at 618 nm (∼5.6 nm CdSe core). Corresponding CdSe/ZnS wet gels were prepared by addition of tetranitromethane, resulting in irreversible loss of surface thiolate groups because of disulfide formation. The resulting wet gels were aged for 7−10 days to form monolithic wet gels with nearly identical photoluminescence (PL) spectra to those of the quantum dot precursors (Figure 1 and Supporting Information). The intense luminescence of these gels is easily detected by the naked eye.

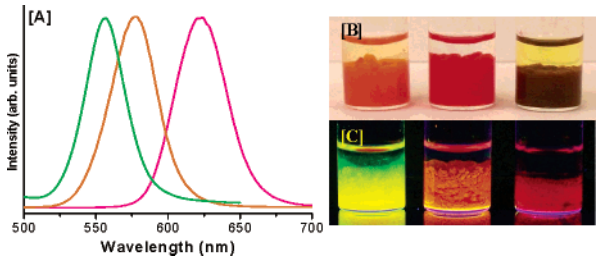

Figure 1. [A] Emission spectra of wet gels prepared from CdSe/ZnS core/shell nanoparticles; photograph of corresponding gels [B] under regular light, and [C] upon UV illumination.

The yellow-green-emitting gels were transformed into aerogels by exchanging the solvent with acetone, followed by supercritical CO_2 drying.[6] The supercritical fluid permits solvent to be removed from the pores without collapse and densification. Alternatively, the acetone exchanged gels were dried on the benchtop to produce xerogels. Assembly and drying is accompanied by a small decrease in sulfur content, from 39 to 36 atom % (nanoparticles vs aerogel), as probed by energy dispersive spectroscopy. This is consistent with the loss of thiolate functionalities during gel formation. The metal/chalcogen ratio in the aerogels is 1:1 with an overall Cd/Zn ratio of 1:3.4, suggesting shell growth was relatively efficient (synthesis composition: 1:4 Cd/Zn). Network formation has no apparent impact on the structure or crystallinity of the primary CdSe/ZnS particles that make up the aerogels and xerogels, as probed by powder X-ray diffraction (Supporting Information). The diffraction pattern of CdSe/ZnS nanoparticles is characteristic of hexagonal CdSe with a slight shift in diffraction peaks ($2\theta \approx 0.2-0.4°$) toward larger 2θ (smaller d-spacing) owing to the compression of the CdSe lattice planes by the ZnS shell.[9] A slightly larger 2θ shift (0.4−0.8°) is found in xerogels and aerogels, presumably due to the increase in thickness and further growth of the ZnS shell upon gelation and aerogel/xerogel formation. This shell growth that accompanies gelation is also evident from transmission electron microscopy (TEM). In contrast to the fine-featured particulate aerogels produced from bare CdSe nanoparticles, the CdSe/ZnS composites appear almost glassy, as if the ZnS shells have fused together to form a matrix embedding the CdSe nanoparticles (Figure 2). A still larger degree of fusion is apparent in the CdSe/ZnS xerogel (Supporting Information).

10.1021/ja066749c CCC: $37.00

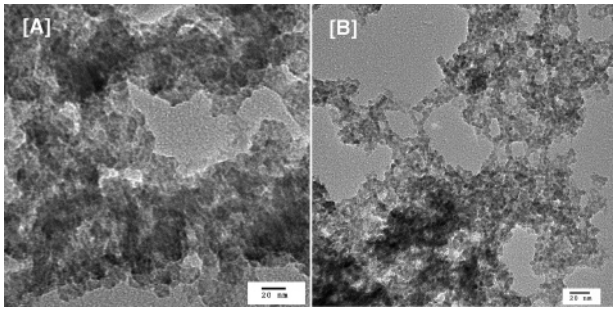

Figure 2. Electron micrographs showing aerogel morphology for [A] CdSe/ZnS and [B] CdSe.[6d] The scale bar is 20 nm.

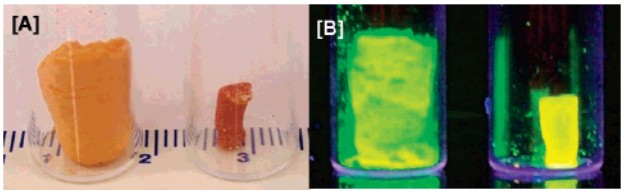

Figure 3. Photograph of CdSe/ZnS aerogels (left) and xerogels (right) under [A] normal and [B] UV illumination.

For both aerogels and xerogels, large (mm−cm) monoliths could be obtained and were highly emissive under UV illumination, just like the wet-gel precursors (Figure 3). The large difference in volume in the two samples is due to the significant compaction of the nanoparticle network in the xerogel, resulting in a 20 fold increase in density for the xerogel (1.7 g/cm^3) relative to the aerogel (0.08 g/cm^3) monolith. This is further reflected in the surface areas and pore characteristics determined from nitrogen adsorption−desorption isotherms on aerogel and xerogel powders (Supporting Information). CdSe/ZnS aerogels exhibited surface areas ranging from 188 to 234 m^2/g for three individually prepared samples, relative to ∼70 m^2/g for xerogels. Pore diameters calculated based on the Barrett−Joyner−Halenda (BJH) model reveal a higher average pore diameter (21−23 nm) for aerogels compared to that of xerogels (7−10 nm), and the aerogels exhibited a broader range of pore sizes in the distribution plot, extending throughout the meso (2−50 nm) and into the macro (>50 nm) regime. The presence of meso- and macropores in the aerogels—and the near absence of >10 nm pores in xerogels—is also evident in TEM micrographs (Figure 2a, Supporting Information).

In contrast to nanostructured networks composed of bare CdSe particles, the density of the CdSe/ZnS network has very little effect on the optical and electronic properties of these materials (Figures 3, 4). Both aerogels and xerogels of CdSe/ZnS exhibit absorption onsets and PL maxima that are similar to the nanoparticle precursors, with the xerogels exhibiting slightly greater breadth. The absence of broad features to the red of the band-edge peak is consistent with the eradication of trap states owing to the encapsulation of CdSe in the ZnS matrix and is responsible for the high luminosity of these monoliths. The PL of CdSe nanoparticles, aerogels and xerogels, on the other hand, is dominated by trap-state emission; band-edge emission is not observed at all for the CdSe xerogel. Likewise, the absorption onset is significantly broadened for the xerogel and extends far into the red, consistent with a lower-degree of quantum confinement owing to enhanced interparticle interactions within the dense network. Thus, maintaining quantum confinement effects in sol−gel prepared metal chalcogenide nanostructured networks can be achieved by either

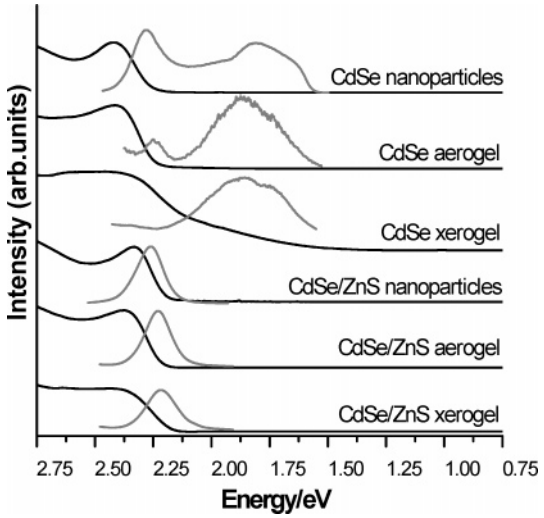

Figure 4. Optical absorption (gel data converted from reflectance, black) and photoluminescence (gray) spectra of CdSe[6d] and CdSe/ZnS samples.

limiting the dimensionality (density) of the network or by introducing spacers between particles to limit interactions. The advantage of the latter strategy is the ability to create highly emissive materials, such as the CdSe/ZnS gels, xerogels, and aerogels presented here, which may be suitable for the manufacturing of LEDs and in optical gain applications.

Acknowledgment. We thank Mercouri Kanatzidis for the use of solid-state optical bandgap equipment. This research was supported in part by a grant from the NSF (Grant DMR-0094273) and the ACS-PRF (Grant 43550-AC10).

Supporting Information Available: Experimental details, X-ray powder diffraction, TEM micrographs, porosimetry plots, and absorbance and photoluminescence data. This material is available free of charge via the Internet at http://pubs.acs.org.

References

(1) (a) Steckel, J. S.; Snee, P.; Coe-Sullivan, S.; Zimmer, J. P.; Halpert, J. E.; Anikeeva, P.; Kim, L.-A.; Bulovic, V.; Bawendi, M. G. *Angew. Chem., Int. Ed.* **2006**, *45*, 5796−5799. (b) Sundar, V. C.; Eisler, H. J.; Bawendi, M. G. *Adv. Mater.* **2002**, *14*, 739−743.
(2) (a) Michalet, X.; Pinaud, F. F.; Bentolila, L. A.; Tsay, J. M.; Doose, S.; Li, J. J.; Sundaresan, G.; Wu, A. M.; Gambhir, S. S.; Weiss, S. *Science* **2005**, *307*, 538−544. (b) Huynh, W. U.; Dittmer, J. J.; Alivisatos, A. P. *Science* **2002**, *295*, 2425−2427. (c) Nazzal, A. Y.; Lianhua, Q.; Peng, X.; Xiao, M. *Nano. Lett.* **2003**, *3*, 819−822.
(3) Trindade, T. O.; O'Brien, P.; Pickett, N. L. *Chem. Mater.* **2001**, *13*, 3843−3858.
(4) Shevchenko, E. V.; Talapin, D. V.; Kotov, N. A.; O'Brien, S.; Murray, C. B. *Nature* **2006**, *439*, 55−59.
(5) (a) Kim, J. Y.; Osterloh, F. E. *J. Am. Chem. Soc.* **2005**, *127*, 10152−10153. (b) Shavel, A.; Gaponik, N.; Eychmüller, A. *Eur. J. Inorg. Chem.* **2005**, 3613−3623. (c) Lee, J.; Govorov, A. O.; Kotov, N. A. *Angew. Chem., Int. Ed.* **2005**, *44*, 7439−7442.
(6) (a) Mohanan, J. L.; Arachchige, I. U.; Brock, S. L. *Science* **2005**, *307*, 397−400. (b) Mohanan, J. L.; Brock, S. L. *J. Non-Cryst. Solids* **2004**, *350*, 1−8. (c) Arachchige, I. U.; Mohanan, J. L.; Brock, S. L. *Chem. Mater.* **2005**, *17*, 6644−6650. (d) Arachchige, I. U.; Brock, S. L. *J. Am. Chem. Soc.* **2006**, *128*, 7964−7971.
(7) Wang, Q.; Iancu, N.; Seo, D.-K. *Chem. Mater.* **2005**, *17*, 4762−4764.
(8) (a) Talapin, D. V.; Rogach, L. A.; Kornowski, A.; Haase, M.; Weller, H. *Nano. Lett.* **2001**, *1*, 207−211. (b) Dabbousi, B. O.; Rodriguez-Viejo, J.; Mikulec, F. V.; Heine, J. R.; Mattoussi, H.; Ober, R.; Jensen, K. F.; Bawendi, M. G. *J. Phys. Chem. B* **1997**, *101*, 9463−9475. (c) Hines, M. A.; Guyot-Sionnest, P. *J. Phys. Chem.* **1996**, *100*, 468−471.
(9) Manna, L.; Scher, E. C.; Li, L.; Alivisatos, A. P. *J. Am. Chem. Soc.* **2002**, *124*, 7136−7145.

JA066749C